



**QUEEN'S
UNIVERSITY
BELFAST**

Lysine-derived, pH-sensitive and Biodegradable Poly(Beta-aminoester Urethane) Networks and Their Local Drug Delivery Behaviour

Tamer, Y., & Chen, B. (2018). Lysine-derived, pH-sensitive and Biodegradable Poly(Beta-aminoester Urethane) Networks and Their Local Drug Delivery Behaviour. *Soft Matter*, 14(7), 1195-1209 .
<https://doi.org/10.1039/c7sm01886j>

Published in:
Soft Matter

Document Version:
Peer reviewed version

Queen's University Belfast - Research Portal:
[Link to publication record in Queen's University Belfast Research Portal](#)

Publisher rights

© 2018 The Royal Society of Chemistry. This work is made available online in accordance with the publisher's policies. Please refer to any applicable terms of use of the publisher.

General rights

Copyright for the publications made accessible via the Queen's University Belfast Research Portal is retained by the author(s) and / or other copyright owners and it is a condition of accessing these publications that users recognise and abide by the legal requirements associated with these rights.

Take down policy

The Research Portal is Queen's institutional repository that provides access to Queen's research output. Every effort has been made to ensure that content in the Research Portal does not infringe any person's rights, or applicable UK laws. If you discover content in the Research Portal that you believe breaches copyright or violates any law, please contact openaccess@qub.ac.uk.

Open Access

This research has been made openly available by Queen's academics and its Open Research team. We would love to hear how access to this research benefits you. – Share your feedback with us: <http://go.qub.ac.uk/oa-feedback>



Lysine-derived, pH-sensitive and Biodegradable Poly(Beta-aminoester Urethane) Networks and Their Local Drug Delivery Behaviour

Received 00th January 20xx,
Accepted 00th January 20xx

DOI: 10.1039/x0xx00000x

Yasemin Tamer^a and Biqiong Chen^{b*}

www.rsc.org/

In this study, a series of covalently crosslinked, L-lysine based poly(beta-aminoester urethane) (LPBAEU) networks with good biodegradability and pH sensitivity were reported. The effect of hydrophilic/hydrophobic character and diacrylate/amine molar ratio on the structure, swelling and degradation behaviour of the networks was investigated. Water transport mechanism and dynamic swelling behavior of LPBAEU networks were strongly affected by medium pH, and swelling amounts up to 252.2% and 148.7% were observed in pH 5.6 and pH 7.4, respectively. It was found that water diffusion within the networks followed non-Fickian mechanism. The LPBAEU network with the highest diacrylate/amine molar ratio exhibited the highest tensile strength and Young's modulus. *In vitro* mass losses of networks showed that the degradation rate of LPBAEU networks can be adjusted from 4 to 14 days. LPBAEU networks also supported loading of doxycycline hyclate (DH) and *in vitro* release studies demonstrated that release of DH from the networks was substantially hindered in the neutral pH environment, with 20.9-56.2% DH release, whereas DH release was accelerated in mild acidic condition, with a release percentage of 36.6-99.6%. The release data were fitted to different mathematical models and obtained results confirmed that these networks released DH in a non-Fickian mechanism. The results of this research support the idea that pH-responsive LPBAEU networks may find potential applications in local drug delivery.

Introduction

In recent years, there has been an increasing amount of literature on the development of non-toxic, biodegradable and biocompatible chemically crosslinked polymer networks for applications such as tissue engineering, drug delivery, artificial skin and microdevices.¹⁻⁴ Numerous polymeric biomaterials containing hydrolyzable bonds to achieve biodegradability have been developed to date including poly(ϵ -caprolactone), poly(lactic-co-glycolide), poly(propylene fumarate), poly(ethylene glycol) and poly(beta-aminoester).⁵⁻⁸ Among them, a considerable amount of literature has been published on poly(beta-aminoester) (PBAE) polymers that are completely biodegradable due to the hydrolysis of their ester bonds.^{9,10} In particular, degradable networks of these PBAE polymers that can be obtained with PBAEs having acrylate end groups, are highly attractive since their properties can be tuned by changing the diacrylate/amine molecules and their ratio to

influence crosslinking density, hydrophilicity and degradation time.^{1,2,11-13} Yet, carcinogenic diacrylates are not generated through degradation since retro-Michael addition reaction is not observed.¹⁰

A current approach on biomaterials development has been on the use of different chemical functionalities in the same structure, in order to control the biocompatibility, degradation rate and mechanical properties for a specific application.^{8,14,15} As a result, many researchers have been focused on poly(ester urethane)s (PEUs) which are degradable with hydrolysable ester groups and have good thermal and mechanical properties due to the strong interactions between their amide groups.^{11,16} This flexible platform, combining the advantages of urethane and ester groups, has great potential as a biomaterial due to their non-toxicity, adjustable biodegradability and capability of creating ionic interactions with biomolecules.¹⁷

However, the adjustment of the properties of these PEUs to meet the biodegradability and biocompatibility requirements is an important issue and thus, novel poly(beta-aminoester urethane)s (PBAEUs) can be synthesized by using diisocyanates generated from amino acids.^{18,19} To this end, there is an expanding interest on the usage of L-lysine diisocyanate (LLDI) in designing new polymers due to its potential hydrolytic degradable product, L-lysine, that is vital and more importantly not detrimental for our living

^aDepartment of Polymer Engineering, Yalova University, Yalova, 77100, Turkey.

^bSchool of Mechanical and Aerospace Engineering, Queen's University Belfast, Ashby Building, Stranmillis Road, Belfast BT9 5AH. Email: b.chen@qub.ac.uk

Electronic Supplementary Information (ESI) available: See DOI: 10.1039/x0xx00000x

system.^{20,21} Zhang and co-workers^{22,23} have developed a series of LLDI-based polyurethanes and found their non-toxic degradation products to be lysine, glycerol (or glucose) and CO₂. Thus, the major advance of LLDI based carriers has been shown to have an easy evacuation by virtue of biodegradability after completing their function in the body.^{24,25}

These crosslinked PBAEU polymer networks might be potential candidates for local drug delivery systems. In particular, local antibiotic delivery for periodontal diseases has become increasingly important during the past several years because of their efficiencies in minimizing the systemic exposure of antibiotics and maximizing the therapeutic efficiency as compared with the systemic delivery that causes adverse drug reactions by oral antibiotic intake.²⁶⁻²⁹ So far, different polymeric carriers exhibiting different release profiles for periodontal purposes have been designed in numerous forms such as microspheres, films, strips, rings, gels and injectable systems.^{30,31} However, only a few studies have focused on the usage of stimuli responsive devices for local antibiotic delivery in the treatment of periodontal diseases. The oral cavity has a pH range between 5.75 and 7.05,²⁶ and inflammation generally causes a relatively acidic environment with a pH value of 6 or less,³² so the usage of a delivery system with pH sensitivity can enhance the effectiveness of treatment. Recently, Yu et al.³³ reported a new generation of pH sensitive and chitosan-based hydrogels and examined the *in vitro* antibiotic release profile of these hydrogels. Owing to the cationic nature, PBAEU polymers are capable of showing pH-responsive behaviour resulting from protonation or deprotonation of their tertiary amino groups in the backbone,^{10,34} and therefore these pH sensitive networks seem to be good candidates for carrying antibiotics in periodontal therapy.

This work aimed to design novel pH sensitive, lysine based poly(beta-aminoester urethane) (LPBAEU) networks with adjustable swelling kinetics and biodegradability for local drug delivery applications. Firstly L-lysine containing urethane diacrylate (LDA) monomer was synthesised, and different types of crosslinkable LPBAEU macromers were obtained by using two different amine and diacrylate molecules and varying their molar ratio. Then, the residual acrylate groups of these macromers were chemically crosslinked via free radical polymerization. The effect of the changes in polymer structure and diacrylate/amine ratio on water diffusion mechanism, swelling and degradation profiles was investigated. Doxycycline hyclate (DH), an antibiotic against a wide spectrum of diseases caused by many gram-positive and gram-negative bacteria, was used as a model drug^{26,35} to examine the drug delivery performance of these polymers for potential treatment of periodontal disease. Also, *in-vitro* DH release mechanism was explored in detail using various mathematical models.

Experimental

Materials

Poly(ethylene glycol) diacrylate (PEGDA) (\bar{M}_n :700), 4,4-trimethylenedipiperidine (TMDP, 97%), 2-aminoethanol (AE, ≥99.5%), 2-hydroxyethyl acrylate (HEA, %96), dibutyltin dilaurate (DBTL, 95%), ammonium persulfate (APS, ≥98.0%), N,N,N,N-tetramethylethylenediamine (TEMED, ≥99%), phosphate buffered saline (PBS) tablets and lipase enzyme form porcine pancreas were purchased from Sigma Aldrich. L-Lysine ethyl ester diisocyanate (LLDI, 97%) and doxycycline hyclate were supplied from Alfa-Aeser. All the solvents, chloroform (CHCl₃), diethyl ether, dichloromethane (DCM), dimethyl sulfoxide (DMSO), tetrahydrofuran (THF) and hexane, were of analytical grade and obtained from Sigma-Aldrich and used as received.

Synthesis

The synthesis of macromers was performed in two steps. For the first step, 1.16 g HEA and 0.0126 g DBTL were dissolved in 20 ml CHCl₃ and exposed to three 10-minute cycles of vacuum drying followed by nitrogen purging. The mixture was heated to 60 °C after the addition of 1.13 g LLDI and reflux under N₂ for 4 hours. The majority of the solvent was evaporated in a rotary evaporator until approximately 10 ml CHCl₃ left and the reaction mixture was precipitated in hexane. The obtained diacrylate product, LDA, was dried under vacuum for 2 days.

The acrylate terminated LPBAEU macromers were obtained by Michael type addition step-wise polymerization between the mixture of LDA and PEGDA and AE or TMDP as reported previously.³⁶ In a typical experiment, a mixture of 2.2 g LDA and 1.54 g PEGDA, and 0.36 g AE monomer were dissolved separately in THF. The diacrylates containing solution was placed into a glass vial and the amine solution was added dropwise and the polymerization was carried out under magnetic stirring at 55 °C for 3 days. The reaction mixture was precipitated into diethyl ether to remove any unreacted monomer and the obtained macromer was dried in a desiccator connected to a vacuum pump for 3 days. Different macromers were obtained by changing the type of amine molecule and the ratio of diacrylate to amine (Table 1).

The LPBAEU networks were obtained by using a chemically initiated free radical polymerization using APS and TEMED as an initiator and catalyst, respectively. First, macromer was dissolved in ethanol at a concentration of 75 wt%, and the mixture of 2 wt% APS (dissolved in 0.5 ml ethanol) and 2 wt% TEMED (based on macromer weight) were added to this solution. The mixture was transferred to a non-sticky mold after being sonicated for 30 s, and kept at room temperature for 2 days and further 2 days under vacuum at 40 °C to realize crosslinking and evaporate the solvent. Specimens with a dimension of 10 mm x 10 mm and a thickness of 0.44 ± 0.08 mm were cut from the films to be used in swelling, degradation and drug release studies.

Table 1 The theoretical composition, molecular weight, sol fraction and contact angle of LPBAEU networks*

Sample	Feed ratio / %				D:A ratio	Yield / %	Molecular weight / g mol ⁻¹			Sol fraction / %	Contact angle / °
	LDA	PEGDA	AE	TMDP			\bar{M}_w	\bar{M}_n	PDI		
LPBAEU-A1	27.28	27.28	45.44	0	1.2:1	89.6	7340	2996	2.45	8.2 ± 0.3	29.8 ± 8.6
LPBAEU-A2	29.17	29.17	41.66	0	1.4:1	91.2	6180	3936	1.57	3.7 ± 0.9	45.5 ± 6.7
LPBAEU-T1	27.28	27.28	0	45.44	1.2:1	87.4	8350	4217	1.98	13.5 ± 0.7	48.6 ± 2.1
LPBAEU-T2	29.17	29.17	0	41.66	1.4:1	88.1	7125	3345	2.13	6.4 ± 0.2	69.3 ± 3.5

*The monomer and polymer names are abbreviated as described in the main text.

Characterization

Chemical structure and physical properties

Attenuated Total Reflectance Fourier Transform Infrared (ATR-FTIR) analysis was done by using a Perkin Elmer Frontier FTIR spectrometer at a resolution of 4 cm⁻¹, in the range of 4000–600 cm⁻¹. The structural elucidation of macromers was done by a 500 MHz Bruker Proton Nuclear Magnetic Resonance (¹H-NMR) spectrometer using CDCl₃ and tetramethylsilane (TMS) as the solvent and internal reference, respectively. The molecular weights of the macromers were measured by Gel Permeation Chromatography (GPC) using a Hewlett-Packard 1090 HPLC with a differential refractive index detector and linear polystyrene standards to calibrate the columns. CHCl₃ was used as eluent at a flow rate of 1.0 mL min⁻¹. The glass transition temperatures (T_g) of LPBAEU networks were tested under nitrogen atmosphere with a Perkin-Elmer Diamond DSC at a rate of 10 °C min⁻¹ in the temperature range between -70 °C and 100 °C. Second heating runs were used to obtain the T_g values. Water-contact angle (CA) measurements of thin crosslinked LPBAEU films that were obtained on glass slides were taken by using a KRÜSS DSA100 contact angle analyser image system. Distilled water was utilized as wetting liquid and five measurements were taken for each sample. To determine the sol fraction, the LPBAEU film specimens (n=3) were immersed in DCM for 24 h and the values were calculated by dividing the mass loss between the initial and the final weight of the dry sample by the initial weight of the sample.

The swelling characteristics of the copolymer films were studied in PBS at two different pH values at room temperature. The swollen films were removed at various time points and immediately weighed after the water on the surface of the film was superficially removed with a tissue. Equilibrium state was considered when no further change was noticed in the weight of the swollen films and the swelling degree, SD, was calculated by using eqn (1):

$$SD(\%) = (M_t - M_0)/M_0 \times 100 \quad (1)$$

where M_t and M_0 stand for the swollen weight of sample at time t and the dry weight of sample, respectively. To obtain more reliable results three experiments were done for each sample. Also, swelling kinetics and water diffusion mechanism of the networks were

determined by using the Voigt model³⁷ and Korsmeyer-Peppas model³⁸ as described in Supporting Information.

Tensile tests were carried out on a Zwick/Roell test machine at a speed of 10 mm min⁻¹, using a 50 N load cell at room temperature. Samples with a rectangular shape (5 mm x 50 mm) were cut from crosslinked films and subjected to tension until failure. The ultimate tensile strength, Young's modulus (determined from the initial slope of the stress/strain curve) and elongation at break were calculated from three measurements for each sample.

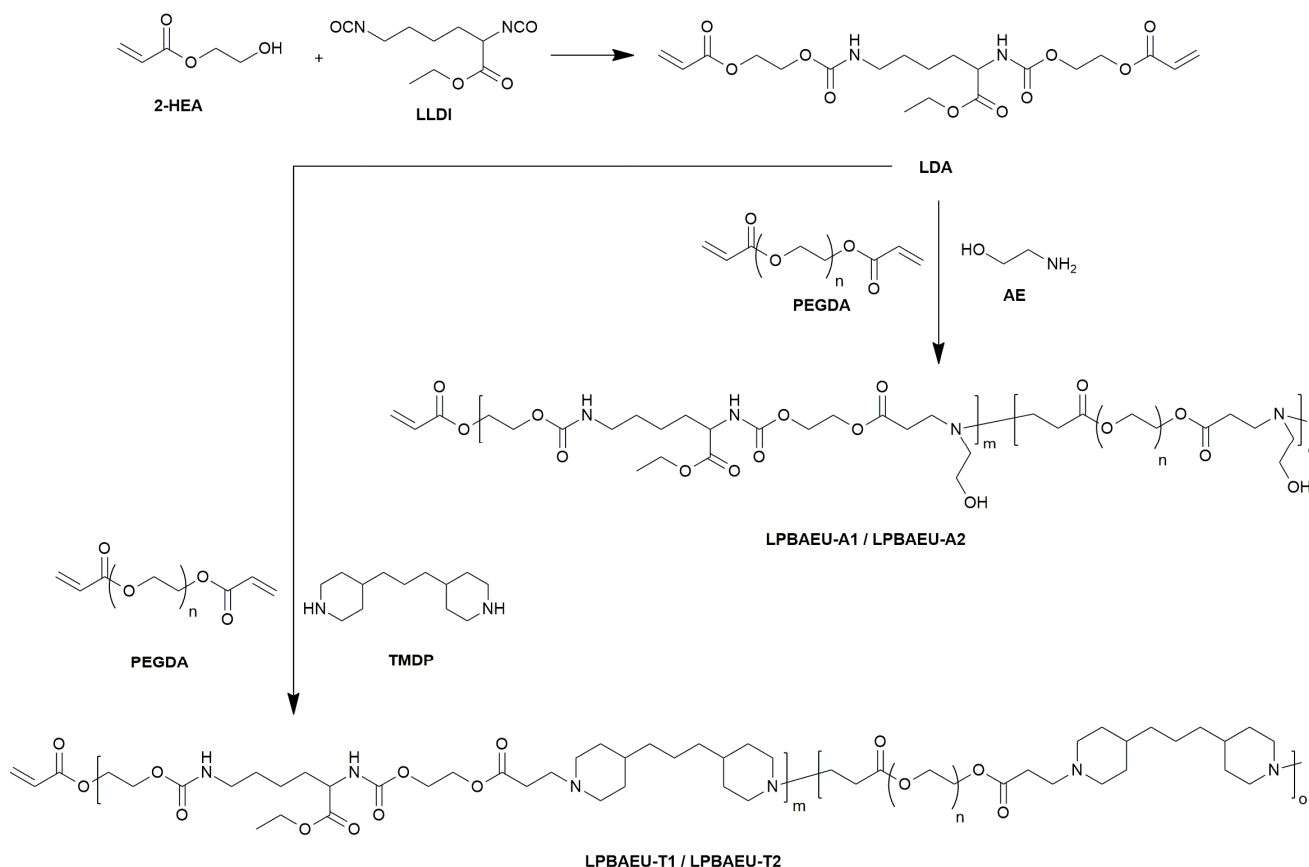
Degradation studies

The *in vitro* degradation studies were performed with and without enzyme, lipase. The films with initial dry weights measured were immersed into 10 mL 0.05 M PBS (pH 7.4) for hydrolytic degradation and 0.1 mg mL⁻¹ lipase containing PBS solution for enzymatic degradation, and the degradation tests were carried out for 14 days in a shaker incubator (Stuart, S1500) at 100 rpm and 37 °C. The PBS/enzyme solution was replaced every 24 h to maintain the same level of enzymatic activity. At predetermined time intervals film samples were collected until they cannot be handled, and were gently washed with distilled water to remove PBS salts and kept under vacuum at 40 °C until a constant weight was reached to determine the remaining mass. Three parallel experiments were carried out for each network films and their mass change was recorded. The degradation ratio was determined by comparison of the weights of the film before and after degradation.

To determine the degradation products of LPBAEU-T1 network, the sample was immersed in distilled water and kept at 37°C in a shaker. After 7 days, the sample was taken out and aliquots of distilled water being in contact with the network were condensed in vacuum at 40°C to obtain degradation products. Then, FTIR-ATR spectrum of the resulting product was taken.

Drug loading and release properties

The drug loaded LPBAEU networks were obtained by soaking the copolymer films in doxycycline hyclate DMSO solution (1 mg mL⁻¹) for 24 h.³⁹ Then, the drug loaded films were washed with PBS to remove the surface adsorbed drug and dried under vacuum for 24 h at 40 °C and stored in desiccator for further study. For *in vitro* drug release studies, the DH-loaded samples were placed in 10 mL PBS solution in neutral (pH 7.4) and mild acidic (pH 5.6) conditions at 37 °C in a shaker incubator (100 rpm). At desired time points, 4 ml of



Scheme 1. Schematic diagram of the synthesis and chemical structures of the polymers.

the solution was removed and replaced with the same amount of fresh PBS to maintain total volume constant. Quantitative analysis of the removed PBS solution was done by measuring the UV absorbance at 346 nm by using a UV spectrometer (Lambda 900, Perkin Elmer) operating at a resolution of 1 nm. To establish the relationship between the drug concentration and absorbance, the standard calibration curve of free DH in PBS at the wavelength of 346 nm was developed ($R^2 = 0.9988$). The quantity of DH released was calculated by comparing the obtained UV-Vis spectra with the standard calibration curve of free DH. All experiments were repeated 3 times. To determine the entrapped drug content in the network film samples, the drug release studies were continued until the samples became brittle. The entrapped DH amount was measured by the same method as described above. The drug loading percentage, LC, was calculated on the basis of the following formula⁴⁰,

$$LC(\%) = w_D/w_{NF} \times 100 \quad (2)$$

where w_D and w_{NF} represent the weights of loaded drug and network film, respectively.

Results and discussion

Structural characterization of LPBAEU macromers and networks

Biodegradable LPBAEU macromers were synthesized by reacting two different diacrylate and amine compounds having different hydrophilic/hydrophobic characteristics as shown in Scheme 1. Briefly, the urethane linkage (-NH-COO-) containing LDA monomer was obtained by the reaction of isocyanate group (LLDI) and hydroxyl group (HEA). Then, LPBAEU macromers were obtained by conjugate addition of the diacrylate to amine for 72 hours at 55 °C, with conversions on the order of 88-91% (Table 1). As a second step, the terminal acrylate groups of these macromers were crosslinked by using APS and TEMED. The ratio of LDA to PEGDA was kept constant at 1:1 in all polymerizations and the total diacrylate to amine molar ratios (D:A ratio) were adjusted to be 1.2:1 and 1.4:1, respectively. Table 1 summarizes the characteristics of the LPBAEUs synthesized at different D:A ratios. Their molecular structure was confirmed using ATR-FTIR and ¹H-NMR techniques as discussed below.

From the FTIR spectrum of LDA (Fig. 1A(b)), the absence of characteristic peak of isocyanate group at 2238 cm^{-1} and the existence of new stretching and bending vibrations of N-H peak at 3321 cm^{-1} and 1535 cm^{-1} indicated the complete reaction of hydroxyl and isocyanate groups and proved the successful synthesis of LDA compound.⁴¹ The absorption bands at around 2800-3000 cm^{-1} are related to the symmetric stretching vibration of the C-H groups. The peak at at 3324 cm^{-1} and the broad absorption band at

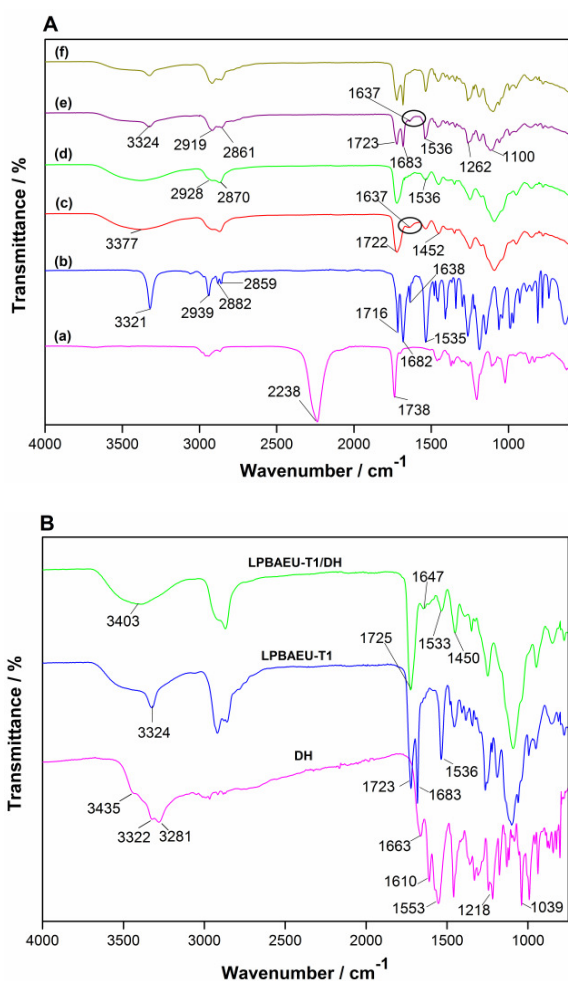


Fig. 1 (A) ATR-FTIR spectra of (a) LLDI, (b) LDA, (c) LPBAEU-A1 macromer, (d) LPBAEU-A1 network, (e) LPBAEU-T1 macromer, (f) LPBAEU-T1 network; and (B) ATR-FTIR spectra of DH and DH-loaded LPBAEU-T1 network.

3377 cm^{-1} are due to the stretching vibration of N–H groups of LPBAEU-T1 and the overlapped stretching vibrations of N–H and O–H groups of LPBAEU-A1, respectively. Since all the NH_2 groups of amine monomers were consumed through the conjugate addition reaction, the observed N–H stretching in the spectra was only due to the urethane structure.⁴² In the carbonyl region of LDA, the obtained peaks at 1716 cm^{-1} and 1682 cm^{-1} are due to the stretching vibrations of the free carbonyl (C=O) of ester and urethane groups.⁴³ In the FTIR spectrum of LPBAEU-T1 network (Fig. 1A(f)) these ester and urethane peaks can be seen very clearly while in the spectrum of LPBAEU-A1 (Fig. 1A(d)), these stretching bands overlapped due to hydrogen bonded carbonyl groups and only one absorption band appears at 1722 cm^{-1} for the carbonyl groups.⁴³ Also, the absorbances at 1536 cm^{-1} and 1262 cm^{-1} are originated from N–H bending and C–N stretching vibrations. From the FTIR spectra of LPBAEU-A1 and LPBAEU-T1 macromers, as shown in Fig. 1A(c,e), the observed absorption peak at 1637 cm^{-1} corresponding to the stretching vibration of terminal acrylate groups (C=C) demonstrated that macromers having acrylate end groups were

formed *via* Michael type addition reaction because of the diacrylate to amine molar ratio exceeding 1.⁴⁴

Fig. 1B compares the FTIR spectra of DH and DH-loaded LPBAEU-T1 network film. Doxycycline hyclate exhibited the following characteristic peaks⁴⁵ at around 3500–3200 cm^{-1} , 1663 cm^{-1} , 1610 cm^{-1} and 1553 cm^{-1} which were assigned to O–H and primary amine N–H stretching vibrations, C=O stretching vibration and N–H bending and C–N stretching vibrations of CONH_2 group, respectively. After DH loading, the peak of 3324 cm^{-1} became wider and flatter, and the region between 3200 and 3600 cm^{-1} represented the overlapping peaks of stretching vibration of O–H and N–H and the enhancement of hydrogen bonding. Also, N–H bending shifted from 1536 to 1533 cm^{-1} , and in carbonyl region, one strong absorption band at 1725 cm^{-1} and a new band at around 1647 cm^{-1} were obtained, corresponding to combined carbonyl stretching of urethane and ester groups.⁴³ These findings suggest the formation of possible hydrogen bonding interactions between the drug and the network through their polar amino, hydroxyl and amide functional groups, as shown in Fig. S1 in Supporting Information.

The samples were analyzed with $^1\text{H-NMR}$ to further confirm the structure and the chemical shifts of characterized protons. The reaction of LLDI and HEA in a ratio of 1:2 resulted in the formation of LDA monomer, as demonstrated by the distinctive peaks in the $^1\text{H-NMR}$ spectrum (Fig. 2a). The peaks of HEA related methylene protons were detected at 4.34 ppm (labeled “b”) while the chemical shifts of methyl and methylene protons in the ethyl ester moiety of LLDI were assigned at 1.36 ppm (labeled “e”) and 4.81 ppm (labeled “d”), respectively.⁴² The aliphatic methylene protons resulting from L-lysine were depicted at 1.52 ppm, 1.50 ppm and 3.18 ppm (labeled “f”, “g+h” and “j”, respectively)³³ and the peak at 3.76 ppm (labeled “c”) related to –CH proton of L-lysine. Characteristic peaks of acrylate end group protons were assigned at 5.85 ppm, 6.19 ppm and 6.46 ppm (labeled “a2”, “a3” and “a1”).³⁴

The spectra in Fig. 2b and 2c indicated the chemical diversity of the LPBAEU-A1 and LPBAEU-T1 macromers. Each $^1\text{H-NMR}$ spectrum with labeled protons exhibited the characteristic signals of LDA monomer, PEG, amines (AE and TMDP) and also terminal acrylate groups. As shown, the distinctive peaks related with the structure of LDA were seen in both of the spectra. In the $^1\text{H-NMR}$ spectrum of LPBAEU-A1 (Fig. 2b), the methylene proton signals attached to hydroxyl group were clearly visible at 2.51 and 3.18 ppm (labeled “m” and “n”) while peaks from 2.61 ppm and 2.83 ppm (labeled “k” and “l”) were related to the methylene protons in the polymeric chain.⁴⁶ The remaining signal near 3.69 ppm (labeled “o”) was linked to the methylene protons of PEG.⁴⁷

In the spectrum of LPBAEU-T1 (Fig. 2c) there were three new signals due to the methyl and methylene protons of TMDP ring at 1.68 ppm and 2.55 ppm (labeled “o”, which overlaps with peak “f” and “m”) and the aliphatic methylene protons of TMDP at 1.36 ppm (labeled “n”).⁴⁷ The $^1\text{H-NMR}$ results confirmed by IR spectra proved that the LDA monomer and the LPBAEU macromers with acrylate end groups were successfully synthesized.

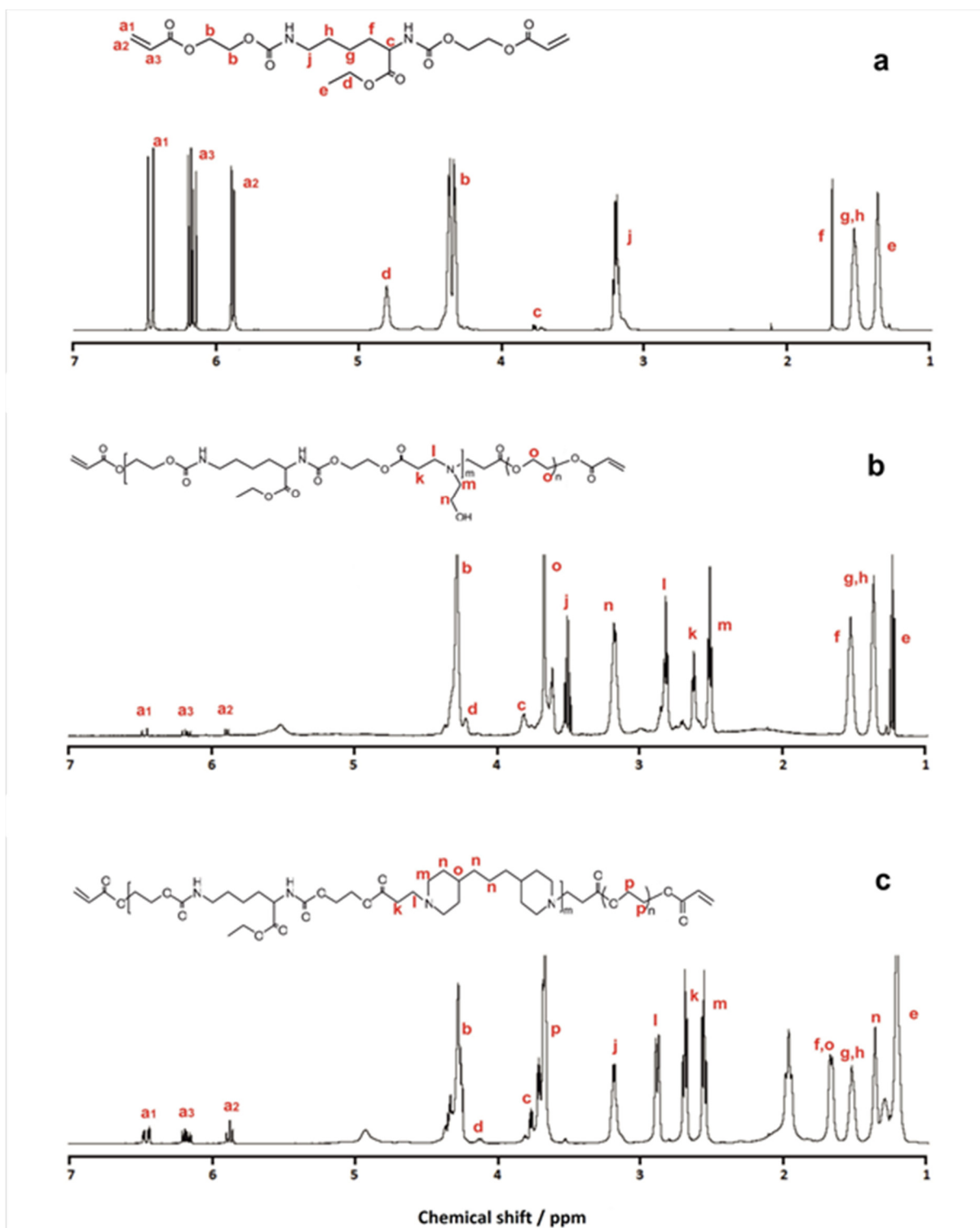


Fig. 2 $^1\text{H-NMR}$ spectra of (a) LDA, (b) LPBAEU-A1 and (c) LPBAEU-T1 macromers.

From the GPC results, the weight average molecular weights of the macromers (\overline{M}_w) were found to be between 6180 g mol^{-1} and 8350 g mol^{-1} relative to polystyrene standards in chloroform (Table 1). Previous studies have showed that step-growth polymerization between diacrylate

and amine monomers controls the molecular weight of the obtained macromer, and the maximum molecular weight is obtained when D:A ratio is 1:1 and the molecular weight decreases as the molar ratio increases.^{1,11} As expected, \overline{M}_w of the resulting LPBAEU macromers decreased with increasing

molar ratio from 1.2:1 to 1.4:1. This polymerization also determines the amount of diacrylate end groups that are responsible for network formation through the subsequent free radical polymerization.¹ Sol fraction is directly related with the double bond conversion of the system and indicates the crosslinking efficiency of the system.¹ In biomedical applications, the sol fraction value of the system is crucial because the released parts can be toxic for the surrounding tissue and also high sol fraction values can adversely affect the final material properties, so the soluble parts must be removed before the application.⁴⁸ The soluble parts in the network structure are likely due to the unreacted macromers with acrylate end groups which are released when the network is swollen in DCM. The sol fraction values showed that the networks with high D:A ratios (low \bar{M}_w) had lower sol fraction values ($\leq 6.4\%$, Table 1). This can be explained by the tendency of lower molecular weight macromers to react faster than the higher molecular weight macromers. Also, the amount of double bonds is greater for higher ratios and this allows lower molecular weight macromers to reach higher double bond conversions and increases crosslinking density.¹

Surface wettability of a biomaterial is of importance to determine the material behaviour in a biological medium, such as surface interaction of polymeric material with cells in the human body.⁴⁹ Therefore, the wettability of the crosslinked networks was identified through water contact angle measurements. The obtained contact angle values of the network films were between 29.8° and 69.3° as given in Table 1, indicating the hydrophilic nature of the networks. It can be observed that the contact angles of LPBAEU-A1/A2 networks are much lower than that of LPBAEU-T1/T2 networks due to the highly hydrophilic characteristic of AE monomer. As D:A ratio increased from 1.2:1 to 1.4:1, the contact angle increased in the same trend due to the increased surface hydrophobicity.

The glass transition temperatures of these crosslinked LPBAEU networks were depicted in Fig. 3. A common feature among the polymeric networks is their low T_g values which are much lower than room temperature, ranging from -52.6°C to -46.6°C . No crystallization or melting peaks were observed for all the samples despite using PEG segments, implying the amorphous nature of the networks. The low molecular weight of PEG segments (700 g mol^{-1}) did not promote crystallization thus resulting in undetectable crystallization peaks (Fig. 3).³⁷ As can be seen from the results, LPBAEU-T2 and LPBAEU-A2 networks (D:A ratio of 1.4:1) showed the highest T_g values because of the reduction in chain mobility of these highly crosslinked structures.⁵⁰⁻⁵²

Swelling studies

The effect of the D:A ratio and the type of the amine molecule on the swelling profile of LPBAEU networks was investigated in PBSs of pH 5.6 and 7.4. As seen in Fig. 4A,B, all networks had similar swelling isotherms; swelling ratio gradually increased with time and then reached an equilibrium state in

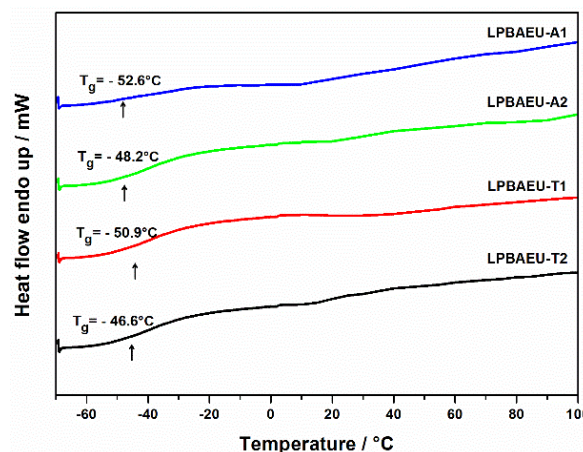


Fig. 3 DSC thermograms of LPBAEU networks. The curves were shifted vertically for clarity.

approximately 6 h for LPBAEU-T2 system and in 3 h for the other systems. It is also apparent that all networks exhibited a pH-responsive swelling, and the equilibrium ratio of swelling in pH 5.6 was higher than that of neutral medium (Fig. 4A,B). The main reason for this is the tertiary amine groups of PBAE polymers with a pK_b value between 5 and 7.2.⁸ The network structure becomes hydrophilic below their pK_b due to the formation of positively charged amine, which allows the formation of H-bonding with water (swollen polymer network), but more hydrophobic at the neutral pH because of the deprotonation of amino groups (compact network structure).⁸ Consequently, all LPBAEU networks showed higher swelling degrees, almost twice, in pH 5.6 in comparison to neutral environment, depending on their structure and D:A ratio.

The interaction between water and LPBAEU networks was mainly determined by the chemical structure of the network, and hydrophilic polymers are more prone to form hydrogen bonds with water molecules and tend to swell to a greater extent.⁵³ From a structural point of view, since AE monomer is more hydrophilic than TMDP, high penetration of water leads to the high swelling ratios up to 252.2% (pH 5.6) for LPBAEU-A1 polymer. Conversely, 166% (pH 5.6) swelling was observed for LPBAEU-T1 due to the reduction in water uptake of this hydrophobic network. The degree of swelling was also dependent on the crosslinking density. As depicted in Fig. 4A,B, maximum swelling ratios of LPBAEU-A2 and LPBAEU-T2 network films were found to be 65.6% and 32.4%, respectively while LPBAEU-A1 and LPBAEU-T1 absorbed 148.7% and 93.4% water at equilibrium at pH 7.4. LPBAEU-A2 and LPBAEU-T2 networks that have high D:A ratio were tightly crosslinked, these rigid and dense structures did not allow large quantities of water to reach the inner parts of the network and hence, the swelling capability was reduced.

Swelling kinetics. The water diffusion into the polymer network causes polymer chain relaxation and subsequently

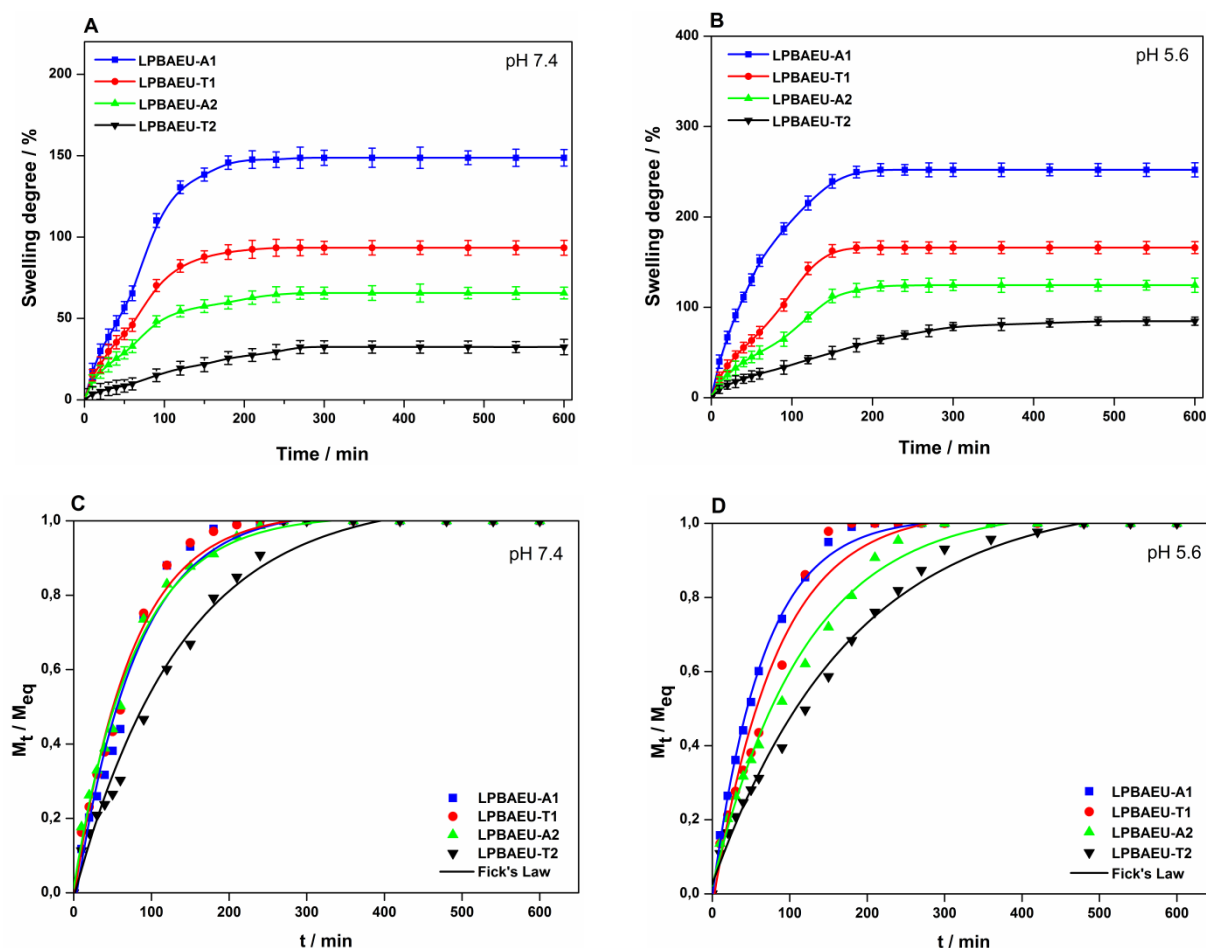


Fig. 4 Swelling properties of LPBAEU networks in (A) pH 7.4 and (B) pH 5.6 PBS solution. The data represented as mean \pm standard deviation ($n=3$). The plot of M_t/M_{eq} as a function of time for LPBAEU network films in (C) pH 7.4 and (D) pH 5.6 PBS solution.

polymeric network to begin expanding in aqueous solution.⁵³ The water diffusion mechanism through the network can be identified based on the Korsmeyer-Peppas power-law expression as shown in Equation 3.^{38,54}

$$\ln\left(\frac{M_t}{M_{eq}}\right) = \ln K + n \cdot \ln t \quad (3)$$

Here, M_t stands for the swelling degree at time t , M_{eq} represents the equilibrium swelling degree, t is the time in seconds, K is a structural/geometric constant used to identify the swelling ability of the networks and n is the diffusion exponent representing the transport mechanism. This equation can be used for both Fickian and non-Fickian transport mechanisms for thin polymer films and is only valid for the initial swelling stages till 60% of the solvent uptake ($M_t/M_{eq} \leq 0.6$).⁵⁴ The diffusion exponent, n determines the type of transport mechanism, i) $n = 0.5$ for Fickian diffusion, ii) $0.5 < n < 1.0$ for non-Fickian diffusion, iii) $n \geq 1.0$ for the relaxation controlled diffusion and iv) $n < 0.5$ for less-Fickian diffusion.³⁸

The plots of M_t/M_{eq} versus t were drawn (Fig. 4C,D) and the obtained diffusion parameters, K and n , were summarized in Table S1†. It is observed that the n values are between 0.725 and 0.535 for pH 7.4 and, 0.741 and 0.588 for pH 5.6, both higher than 0.5, indicating non-Fickian behaviour of the networks in both solutions. Thus, the penetration rate and polymer relaxation rate control the overall water uptake. The obtained determination coefficient, R^2 , values are above 0.99, indicating the excellent model fitting. It is also apparent from Table S1† that the n values decreased constantly with decreasing hydrophilic characteristic of the network in both cases, pH 5.6 and 7.4, and that n values are higher for low pH value.

Voigt model³⁷ was further used to determine the rate of water diffusion into the LPBAEU networks at pH 5.6 and 7.4 as given in Equation 4.

$$S_t = S_e (1 - e^{-t/\tau}) \quad (4)$$

where S_t and S_e are the swelling rate at time t and the equilibrium swelling rate, respectively. τ (min) is the rate

parameter that is a measure of the swelling rate and low τ values indicates higher swelling rates. It is apparent that, the diffusion rate, τ , values are lower at neutral medium compared to pH 5.6 medium (Table S1[†]). Among the networks, LPBAEU-T2 has the lowest swelling rate and the highest τ value because of its highest D:A ratio.

Mechanical properties

LPBAEU networks need to possess sufficient mechanical strength to be used in local drug delivery applications. Therefore, the ultimate tensile strength, Young's modulus and elongation at break of LPBAEU crosslinked network films were determined and the results are given in Table 2. It can be seen that the ultimate tensile strength and Young's modulus of the networks increased whereas the elongations at break decreased significantly with increasing D/A ratio from 1.2/1 to 1.4/1. LPBAEU-T2 network having D/A ratio of 1.4/1 possessed highest tensile strength (1.4 ± 0.18 MPa), which is 1.8 times higher than that of LPBAEU-A1 network with D/A ratio of 1.2/1. The increase in D/A ratio led to an increase in the crosslinking density of the network films. This generally decreases the ductility (elongation at break) of the films and the networks became more rigid and brittle in nature. On the

Table 2 Mechanical properties of LPBAEU networks.

Sample	Tensile Strength / MPa	Elongation At Break / %	Young's Modulus / MPa
LPBAEU-A1	0.5 ± 0.19	40.7 ± 1.19	1.2 ± 0.61
LPBAEU-A2	1.1 ± 0.15	19.2 ± 0.12	5.7 ± 0.46
LPBAEU-T1	0.7 ± 0.04	32.9 ± 0.21	2.1 ± 0.57
LPBAEU-T2	1.4 ± 0.18	12.0 ± 0.49	9.7 ± 0.38

other hand, at the same D/A ratio (1.2/1 or 1.4/1), lower tensile strength and Young's modulus values were obtained for LPBAEU-A1 and LPBAEU-A2 compared to their counterparts, LPBAEU-T1 and LPBAEU-T2. This can be explained with the differences in their structure, as LPBAEU-A1 or LPBAEU-A2 has more flexible structure due to its composition.

These properties are comparable to pH-sensitive poly(vinyl alcohol) and poly(γ -glutamic acid) hydrogel drug delivery systems and crosslinked PEO hydrogel films reported in the literature.^{55,56}

Hydrolytic and Enzymatic Degradation

The polymeric carrier must undergo controlled degradation to yield water soluble non-cytotoxic breakdown products that subsequently are excreted from the body after completing their biological functions (i.e. releasing the drug).⁵⁷ Previous studies have demonstrated that PBAE based polymers are prone to degradation due to highly hydrolytic susceptibility of the ester linkages, and the polymeric chains are cleaved into fragments to form lower molecular weight degradation byproducts, like bis(beta-amino acid)s.^{11,48} The stability of the urethane bond under physiological

conditions is controversial; some studies have shown the hydrolysis of lysine-derived polymers to yield lysine,^{22,23} while others have reported that the degradation of urethane linkages can only be achieved by enzyme.^{58,59}

To investigate the effect of hydrophilic/hydrophobic characteristic of amine monomer and the D:A ratio on the physiological stability of chemically crosslinked LPBAEU network films, *in vitro* degradation studies were performed in the presence and absence of lipase. The weight losses of the LPBAEU polymers during degradation in PBS are shown in Fig. 5A,B. Comparing these two graphs, it can be seen that the degradation rates of all the network films increased in case of enzymatic degradation verifying that the hydrolysis of ester and urethane bonds can be enhanced with the addition of lipase from porcine pancreas that has reported previously to have effect on ester and urethane degradation.⁶⁰

Among the samples, LPBAEU-T2 network has the lowest degradation rate, so in 14 days, before becoming fragile, 48.7% and 65.3% mass losses were observed after hydrolytic and enzymatic degradation, respectively. The tight network structure of LPBAEU-T2 (D:A ratio of 1.4:1) has protected the ester bonds by reducing the water penetration, and thus led to the slow degradation. However, LPBAEU-A1 and LPBAEU-T1

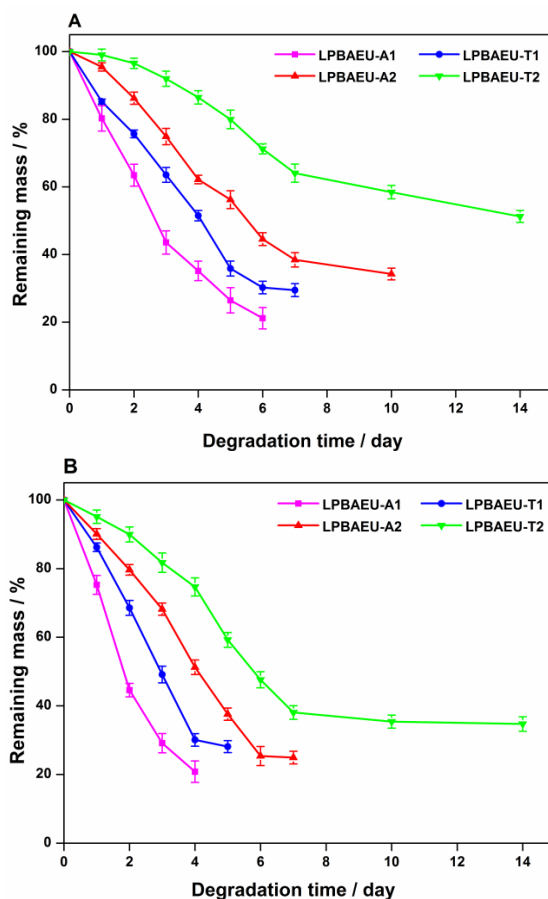


Fig. 5 In vitro degradation profile of LPBAEU network films in PBS solution during (A) hydrolytic and (B) enzymatic degradation at 37 °C. The data represented as mean \pm standard deviation ($n=3$).

networks that have a molar ratio of 1.2:1 degraded much faster; the network films became thin, fragile and nearly 78.8% and 70.5% of weight losses were obtained in PBS without lipase within 6 or 7 days, respectively and almost the same weight loss within 4 or 5 days in case of enzymatic degradation (Fig. 5). This is to be expected because lightly crosslinked networks allow the penetration of large quantities of water and thus, accelerate the degradation. In summary, all LPBAEU networks degraded easily because of their amorphous structure and lower glass transition temperature which facilitate the diffusion of water into the structure and makes them more susceptible to degradation.⁵² Additionally, the networks with quick degradation are consistent with the networks with high swelling degrees.

To analyze the degradation profile of the LPBAEU networks, FTIR studies were carried out, and the FTIR spectra of the LPBAEU-T1 network during degradation were given in Fig. 6A. Degradation of the network has resulted in changes which can be traced by differences in three regions of the FTIR spectra. In region I, the

broad absorption band at 3324 cm^{-1} , corresponding to the stretching vibration of N-H group shifted to the left side of the spectrum after 5 days and its intensity was decreased, while this band was replaced by a broad signal at 3600 cm^{-1} referring two characteristic groups, O-H and N-H, on day 7 (Fig. S2A[†]). In region II, the peak at 1723 cm^{-1} characterizes C=O stretching vibrations in ester structure, while the peak at 1683 cm^{-1} corresponds to N-C=O stretching vibration in the urethane group (Fig. S2B[†]). No visible change was observed after 3 days of degradation, while, after 5 days, the bond at 1683 cm^{-1} disappeared and a new broad peak was formed at 1722 cm^{-1} , indicating the disintegration of urethane bond into carboxylic acid-terminated lysine structure as a result of hydrolysis. In region III, the absorbances at 1536 cm^{-1} and 1264 cm^{-1} could be attributed to N-H bending and C-N stretching vibration in the -C-NH group. On the fifth day of study, the sharp peak at 1536 cm^{-1} appeared as a wide, broad peak, indicating the decreased intensity of N-H bond. After 7 days, this peak shifted to 1546 cm^{-1} and became broader by overlapping with other peaks. Also, the decrease in the intensity of C-N peak and shifting of the peak to

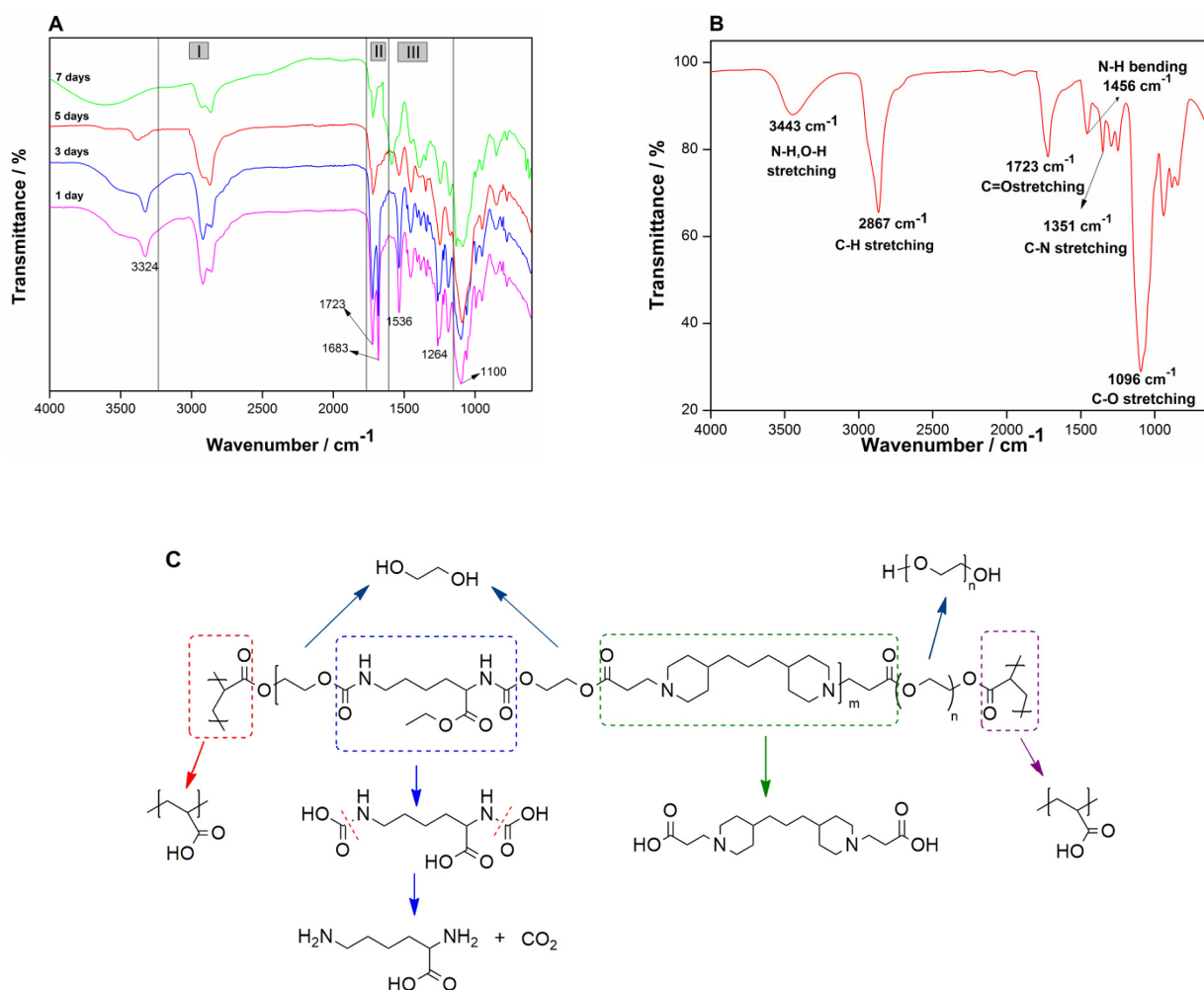


Fig. 6 ATR-FTIR spectra of (A) LPBAEU-T1 network during degradation, (B) degradation products of LPBAEU-T1 network after 7 days degradation, and (C) Potential degradation products of crosslinked LPBAEU-T1 network.

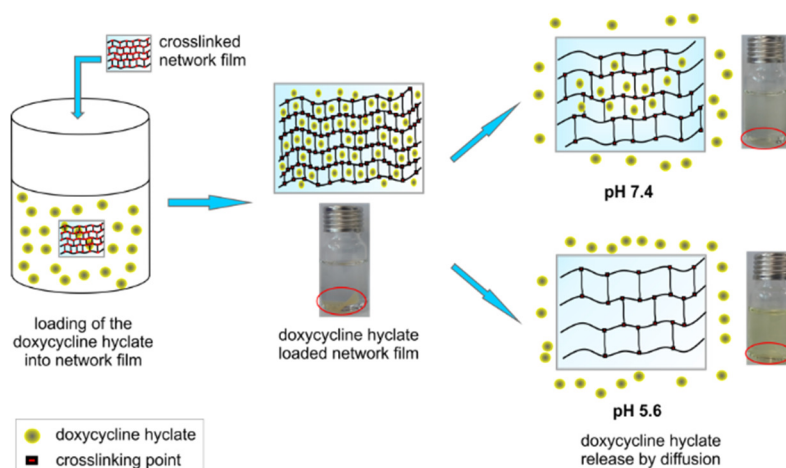


Fig. 7 Schematic diagram illustrating the loading of doxycycline hyclate into the network films and in vitro release in acidic pH (pH 5.6) and physiological pH (pH 7.4). The pictures show the doxycycline hyclate loaded LPBAEU-A1 film after loading and maintained within PBS of pH 7.4 and at pH 5.6 for 72 hours.

1248 cm^{-1} indicated the reduction in C-N bond (Fig. S2C[†]).

The structures of proposed degradation products of LPBAEU-T1 networks are shown in Fig. 6C and the FTIR spectra of these degradation products are given in Fig. 6B.⁶¹ The obtained absorption bands can be described as: the broad band at 3443 cm^{-1} representing N-H and O-H stretching; at around 2867 cm^{-1} representing asymmetric and symmetric C-H stretching in hydrocarbon groups; at 1723 cm^{-1} representing C=O stretching in carboxyl group; at 1456 and 1351 cm^{-1} representing N-H bending and C-N stretching; and at around 1096 cm^{-1} representing C-O stretching vibrations. Consequently, the analysis of both FTIR spectra showed the loss of urethane structures and the formation of new degradation products such as dicarboxylic acid, poly(acrylic acid) and lysine as shown in Fig. 6C.

The degradation products of most synthetic polymers create an acidic environment that can cause inflammation at the implant site, and hence not desirable for most application areas.⁶² In order to examine the effect of degradation products on the pH of the surrounding medium, the pH of the degradation solutions was measured and the results were given in Fig. S3[†]. As can be clearly seen in these figures, the pH of both media changed from 7.4 to 6.9 during degradation, and thus indicated that the breakdown products do not significantly affect the pH value of the degradation medium.

In vitro doxycycline hyclate release study

Doxycycline hyclate was physically adsorbed on the network structure by swelling the polymeric films with drug solution (Fig. 7) and the drug loading percentages of LPBAEU-A1, LPBAEU-A2, LPBAEU-T1 and LPBAEU-T2 networks were found to be approximately 8.0 ± 0.8 wt%, 6.9 ± 1.6 wt%, 7.1 ± 0.4 wt% and 6.3 ± 1.7 wt%, respectively. Fig. 8 demonstrates the in vitro DH release profiles of the network films in two different pH media at 37 °C. Also, the daily doses of released DH on certain

days of the study were given in Fig. S4[†] and Fig. S5[†]. It is obvious that the release rate of DH is higher in mild acidic medium with pH 5.6 than that of neutral medium as shown schematically in Fig. 7. Upon exposure to medium with pH 5.6, the protonation of tertiary amino groups led to repulsion of PBAE chains between two adjacent crosslinking points inside the network structure and all networks swelled to a greater extent and thus increased the drug diffusion from the network.^{63,64} Higher swelling ratios at pH 5.6 created more surface for drug to diffuse from the network to the medium.

All networks showed an initial burst release that could be caused by the washing out of physically entrapped DH molecules that were on or close to the sample surface⁶⁵ (50 mg ml^{-1} water solubility⁶⁶). This effect was seen very clearly in hydrophilic LPBAEU-A1 (initial release of $451 \text{ } \mu\text{g ml}^{-1}$) network which caused the highest water uptake and all drug content was released in medium of pH 5.6 within the first 6 hours (Fig. 8B). This network with high initial DH concentrations might be useful to prevent rapid bacterial growth in short time.²⁶ The weakest burst effect was observed for LPBAEU-T2 network and only 5.4% of loaded DH ($74 \text{ } \mu\text{g ml}^{-1}$) was released in the initial stage as a burst. It is worth noting that this lower DH amount is still above the minimum inhibitory concentration (MIC, $6 \text{ } \mu\text{g ml}^{-1}$ for doxycycline) for most pathogenic bacteria.⁶⁶ The daily doses of DH gradually decreased and then it continued to release DH in a more sustained manner ($\sim 36.6 \pm 3.4\%$ release after 72 h, pH 5.6). Moreover, in case of the networks LPBAEU-T1 and LPBAEU-A2, which differ in the molecular structure and molar ratio, presented almost the same drug release profile and they released 88.6% ($1.36 \text{ } \mu\text{g ml}^{-1}$) and 75.9% ($1.23 \text{ } \mu\text{g ml}^{-1}$) of the loaded drug, respectively (after 72 h, pH 5.6) (Fig. 8B).

Drug Release Mechanism. A single model cannot successfully explain the release behaviour of drug from a network; hence various well-known mathematical kinetic models have been used. Initially, doxycycline hyclate release kinetics from LPBAEU networks

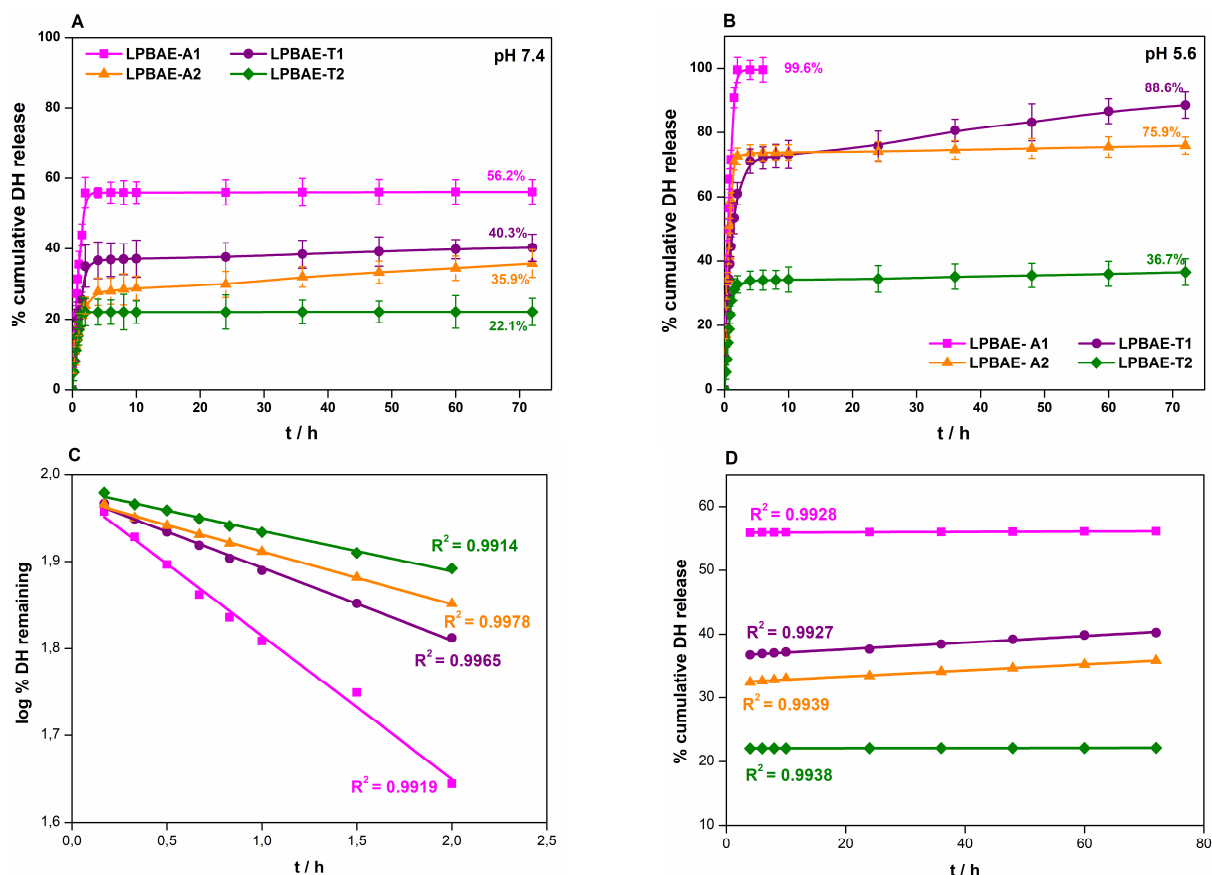


Fig. 8 In vitro release profiles of doxycycline hyclate from the networks in PBS at (A) pH 7.4 and (B) pH 5.6. (Error bars represent the mean \pm SD ($n=3$)). Fitting in-vitro DH release data to (C) first-order release for early time and (D) zero-order release for late time at pH 7.4.

were studied by fitting into zero-order⁶⁷ and first-order kinetic models⁶⁸ (Supporting Information). The best release model was chosen by taking into account the correlation coefficient (R^2) values. The models were applied separately to the early and latter DH release and the obtained R^2 values (Fig. 8C,D and Fig. S6†) showed that the early DH release followed the first order kinetics while the later phase fitted better to zero-order kinetics for both pH media.

Drug release from a polymeric network follows three main steps; first the hydration of the network, then the relaxation or erosion of the network and finally, dissolved drug transportation to dissolution medium through Fickian, non-Fickian or case II diffusion mechanism.⁶⁹⁻⁷¹ To clarify the doxycycline hyclate release mechanism from LPBAEU networks, the release data was also analysed by using the Korsmeyer–Peppas model⁷² that gives main idea for drug release mechanism, the nonlinear Kopcha model⁷³ the Higuchi model⁷⁴ and the Hixson–Crowell model⁷⁵ which clarify the mechanism, defined by the following equations (Eq. 5-8).

Korsmeyer–Peppas model:

$$\frac{M_t}{M} = k \cdot t^n \quad (5)$$

Higuchi model:

$$Q_t = Q_0 + K_H t^{1/2} \quad (6)$$

Hixson–Crowell model:

$$W_0^{1/3} - W_t^{1/3} = K_{HC} t \quad (7)$$

Kopcha model:

$$Q_t = A t^{1/2} + Bt \quad (8)$$

where M_t and M are the quantity of released drug at time “ t ” and the total quantity of drug loaded to the network; Q_t and Q_0 are the quantity of drug release at time “ t ” and the initial quantity of drug in solution; W_0 and W_t are the initial quantity of drug in polymeric matrix and the quantity of drug release at time t and Q_t is the cumulative quantity of drug release at time “ t ”. k , K_H and K_{HC} are the characteristic constants of this polymer and drug system in Korsmeyer–Peppas, Higuchi and Hixson–Crowell models, respectively. Also, the diffusional exponent, ‘ n ’ value can be used to characterize the drug release mechanism of the system as explained in swelling kinetic model. ‘ A ’ and ‘ B ’ are the constants that indicates the contribution of diffusion and erosion in Kopcha model. The higher ‘ A ’ values suggest that Fickian diffusion is mainly responsible for the drug release while the higher ‘ B ’ values indicate

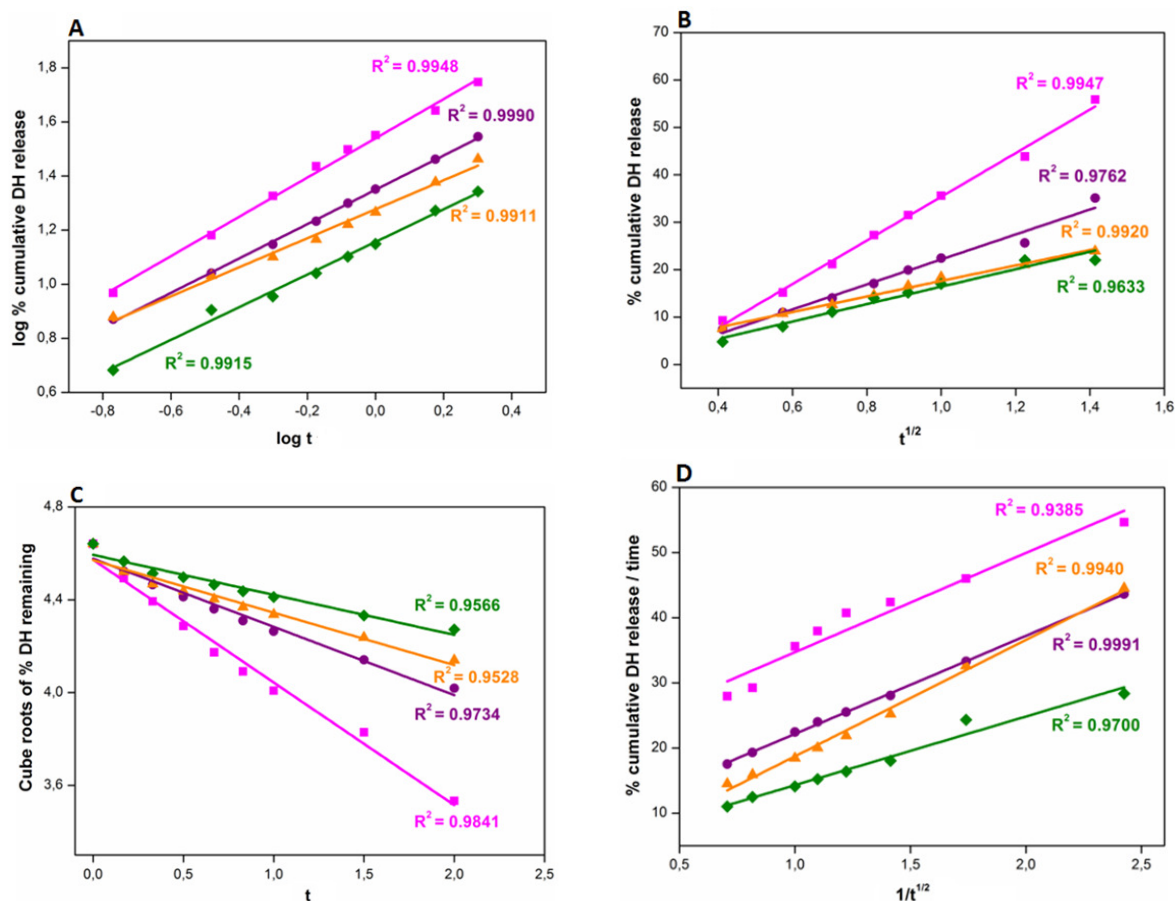


Fig. 9 Fitting the *in-vitro* DH release data to different mathematical models at pH 7.4. (A) Korsmeyer-Peppas model, (B) Higuchi model, (C) Hixson-Crowell model, and (D) Kopcha model. ■: LPAEU-A1, ●: LPAEU-T1, ▲: LPAEU-A2, ◆: LPAEU-T2. The unit of time is hour.

that network erosion is dominant in drug release mechanism.⁷¹ These models fitted well to the first 60% of drug release (early time approximation).⁷⁶

From the analysis of the results, the best fitting was achieved for Korsmeyer-Peppas model and the diffusion exponent (n) values obtained from this model for the initial DH release were found to be $0.54 < n < 0.73$ for pH 7.4 and $0.55 < n < 0.73$ for pH 5.6 (Table S2[†]) implying non-Fickian release mechanism as proven in swelling studies. It clarifies that drug diffusion rate and polymer chain relaxation rate, i.e., erosion of the network, are comparable for these DH loaded LPBAEU network systems.⁷⁷ To further confirm the DH release, nonlinear Kopcha model that gives detailed information about the diffusion (A exponent) and erosion (B exponent) contributions was used. The data fitting was shown in Fig. 9 and Fig S7[†]. The correlation coefficients of Kopcha model showed that both diffusion and erosion had contributions for this non-Fickian pattern; however, the obtained B values were higher than A values, i.e., the A/B ratios were lower than 1 (Table S2[†]), confirming that erosion of network is mainly responsible for drug release at both pH values. As it can be seen from the table, with decreasing pH value (pH 5.6), the ratio of A/B decreased, showing a growing contribution of the erosion effect due to a higher degree of swelling of the network

structures. This effect is particularly significant for highly hydrophilic LPBAEU-A1 and LPBAEU-A2, as well as less dense LPBAEU-T1, so the drops in their A/B ratio were more remarkable and hence lower A/B ratios were obtained compared to that of LPBAEU-T2. In contrast, LPBAEU-T2 possessed a dense network structure which restricted the erosion effect, and hence the highest A/B ratio was achieved among the four networks investigated. As shown in Fig. 9 and Fig S7[†], the lowest R^2 values of LPBAEU-A1 ($R^2=0.9385$) for pH 7.4 and LPBAEU-T2 ($R^2=0.9287$) for pH 5.6 implied the lowest conformity of these networks to the Kopcha model at the said pH condition. Also the R^2 values obtained from Hixson-Crowell and Higuchi models indicated that Higuchi model had a better fitting than Hixson-Crowell model for DH release.

Moreover, these observations were further supported by the diffusion coefficient (D) values of the networks that is also an important penetration parameter to characterize the systems.⁷⁷ D values can be determined by Equation 9, using n and K values.

$$D^n = \frac{K}{4} (\pi l^2)^n \quad (9)$$

where l is the thickness of the initial network films. The D values of networks increased with decreasing pH from 7.4 to 5.6 (Table S3[†]). This suggests that the diffusion of DH molecules from networks is

faster at lower pH than neutral medium. At neutral medium, the diffusion of water molecules in the network is lower, which makes the release rate slower, whereas, at pH 5.6, the observed higher swelling rate led to increased drug release rate. It has also been noticed that the D values for LPBAEU-T2 is lowest out of various networks, which is attributed to its high molar ratio and hence, it's higher degree of hydrophobicity.

Conclusion

A range of novel chemically cross-linked L-lysine based poly(beta-aminoester urethane) polymers were successfully synthesized through Michael type addition reaction followed by free radical polymerization. Their chemical and physical features were adjusted by altering the hydrophilic character of the amine and molar ratios of diacrylate to amine. The obtained equilibrium swelling ratios were essentially depended on the medium pH, and the swelling tests revealed that these crosslinked network films had the ability to absorb water through non-Fickian diffusion model. According to the tensile data, a higher D/A ratio imparted stiffness to the network structure and the networks became more rigid. The obtained *in vitro* mass loss of LPBAEU network films demonstrated that the networks with high molar ratio degraded both hydrolytically and enzymatically and more slowly due to the difficulty in permeation of water through a tortuous path of the tight network. Furthermore, the network films were successfully loaded with doxycycline hyclate through swelling. The release tests demonstrated different drug release profiles for the LPBAEU networks in neutral and acidic incubation media with a reduction of released drug amount during the neutral test, showing a pH sensitive release functionality. Drug release mechanism was also investigated in depth using zero order, first order, Korsmeyer-Peppas, Kopcha, Higuchi and Hixson-Crowell models. The obtained results showed that drug release followed the non-Fickian type diffusion mechanism through erosion of the network. Consequently, these results confirm that the synthesized biodegradable and pH sensitive LPBAEU based crosslinked networks have the potential to be used in local antibiotic delivery applications.

Conflicts of interest

There are no conflicts to declare.

References

- 1 D. L. Safranski, M. A. Lesniewski, B. S. Caspersen, V. M. Uriarte and K. Gall, *Polymer*, 2010, **51**, 3130–3138.
- 2 A. M. Hawkins, T. A. Milbrandt, D. A. Puleo and J. Z. Hilt, *Acta Biomater.*, 2011, **7**, 1956–1964.
- 3 D. Das, P. Ghosh, A. Ghosh, C. Haldar, S. Dhara, A. B. Panda and S. Pal, *Appl. Mater. Interfaces*, 2015, **7**, 14338–14351.
- 4 B. Baroli, *J. Chem. Technol. Biot.*, 2006, **81**, 491–499.
- 5 C. T. Huynh, S. W. Kang, Y. Li, B. S. Kim and D. S. Lee, *Soft Matter*, 2011, **7**, 8984–8990.
- 6 R. Langer and N. A. Peppas, *AIChE Journal*, 2003, **49**, 2990–3006.
- 7 M. S. Matuszowicz, J. Łukaszczyk, R. Pilawka, M. Basiaga, M. Bilewicz and D. Kusz, *Int. J. Polym. Mater.*, 2017, **66**, 1–11.
- 8 B. D. Ulery, L. S. Nair, and C. T. Laurencin, *J. Polym. Sci. B Polym. Phys.*, 2011, **49**, 832–864.
- 9 D. M. Lynn and R. Langer, *J. Am. Chem. Soc.*, 2000, **122**, 10761–10768.
- 10 D. Shenoy, S. Little, R. Langer and M. Amiji, *Mol Pharm.*, 2005, **2**, 357–366.
- 11 D. G. Anderson, C. A. Tweedie, N. Hossain, S. M. Navarro, D. M. Brey, K. J. Van Vliet, R. Langer and J. A. Burdick, *Adv. Mater.*, 2006, **18**, 2614–2618.
- 12 D. L. Safranski, D. Weiss, J. B. Clark, B. S. Caspersen, W. R. Taylor and K. Gall, *J. Biomed. Mater. Res. A*, 2011, **96**, 320–329.
- 13 A. M. Hawkins, D. A. Puleo and J. Zach Hilt, *J. Appl. Polym. Sci.*, 2011, **122**, 1420–1426.
- 14 F. Khan, M. Tanaka and S. R. Ahmad, *J. Mater. Chem. B*, 2015, **3**, 8224–8249.
- 15 R. Langer and D. A. Tirrell, *Nature*, 2004, **428**, 487–492.
- 16 A. Kiziltay, A. M. Fernandez, J. S. Roman, V. Hasirci and N. Hasirci, *J. Biomater. Tissue Eng.*, 2012, **2**, 143–153.
- 17 C. T. Huynh, M. K. Nguyen, J. H. Kim, S. W. Kang, B. S. Kim and D. S. Lee, *Soft Matter*, 2011, **7**, 4974–4982.
- 18 Z. Y. Jian, J. K. Chang and M. D. Shau, *Bioconjugate Chem.*, 2009, **20**, 774–779.
- 19 G. Ciardelli, A. Rechichi, P. Cerrai, M. Tricoli, N. Barbani and P. Giusti, *Macromol. Symp.*, 2004, **169**, 261–272.
- 20 A. M. Fernandez, G. A. Abraham, J. L. Valentin and J. S. Roman, *Polymer*, 2006, **47**, 785–798.
- 21 Z. Wang, L. Yu, M. Ding, H. Tan, J. Li and Q. Fu, *Polym. Chem.*, 2011, **2**, 601–607.
- 22 J. Y. Zhang, E. J. Beckman, N. P. Piesco and S. Agarwal, *Biomaterials*, 2000, **21**, 1247–1258.
- 23 J. Y. Zhang, E. J. Beckman, J. Hu, G. G. Yang, S. Agarwal and J. O. Hollinger, *Tissue Eng.*, 2002, **8**, 771–785.
- 24 D. A. Chiappetta and A. Sosnik, *Eur. J. Pharm. Biopharm.*, 2007, **66**, 303–17.
- 25 C. Yang, A. B. Attia, J. P. Tan, X. Ke, S. Gao, J. L. Hedrick and Y. Y. Yang, *Biomaterials*, 2012, **33**, 2971–2979.
- 26 A. K. Kasperczyk, P. Dobrzynski, M. Pastusiak, B. Jarzabek and W. Prochwicz, *Int. J. Pharm.*, 2015, **491**, 335–344.
- 27 A. C. S. Re, M. P. Ferreira, O. Freitas and C. P. Aires, *Biofouling*, 2016, **32**, 1061–1066.
- 28 H. Hau, R. Rohanizadeh, M. Ghadiri and W. Chrzanowski, *Drug Deliv. and Transl. Res.*, 2014, **4**, 295–301.
- 29 S. P. Noel, H. Courtney, J. D. Bumgardner, and W. O. Haggard, *Clin. Orthop. Relat. Res.*, 2008, **466**, 1377–1382.
- 30 A. Bogren, R. P. Teles, G. Torresyap, A. D. Haffajee, S. S. Socransky and J. L. Wennström, *J. Periodontol*, 2008, **79**, 827–835.
- 31 K. Higashi, M. Matsushita, K. Morisaki, S. Hayashi and T. Mayumi, *J. Pharmacobiodyn.*, 1991, **14**, 72–81.
- 32 W. L. Chiang, Y. C. Hu, H. Y. Liu, C. W. Hsiao, R. Sureshbabu, C. M. Yang, M. F. Chung, W. T. Chia and H. W. Sung, *Small*, 2014, **10**, 4100–4105.
- 33 M. C. Yu, C. Y. Chang, Y. C. Chao, Y. H. Jheng, C. Yang, N. Lee, S. H. Yu, X. H. Yu, D. M. Liu and P. C. Chang, *J. periodontal*, 2016, **87**, 742–748.

- 34 Y. Tamer, H. Yildirim, *Polym. Adv. Technol.*, 2015, **26**, 399–407.
- 35 L. A. Moura, F. V. Ribeiro, T. B. Aiello, E. R. Duek, E. A. Sallum, F. H. N. Junior, M. Z. Casati and A. W. Sallum, *J. Biomater. Sci., Polym. Ed.*, 2015, **26**, 573–584.
- 36 C. T. Huynh and D. S. Lee, *Colloid Polym. Sci.*, 2012, **290**, 1077–1086.
- 37 V. Rana, P. Rai, A. K. Tiwari, R. S. Singh, J. F. Kennedy and C. J. Knill, *Carbohydr. Polym.* 2011, **83**, 1031–1047.
- 38 N. A. Peppas and N. M. Franson, *J. Polym. Sci. Polym. Phys. Ed.*, 1983, **21**, 983–997.
- 39 A. M. Hawkins, N. S. Satarkar and J. Z. Hilt, *Pharm. Res.*, 2009, **26**, 667–673.
- 40 N. Panith, A. Assavanig, S. Lertsiri, M. Bergkvist, R. Surarit and N. Niamsiri, *J. Appl. Polym. Sci.*, 2016, **133**, DOI: 10.1002/APP.44128
- 41 J. Han, B. Chen, L. Ye, A. Y. Zhang, J. Zhang and Z. G. Feng, *Front. Mater. Sci. China*, 2009, **3**, 25–32.
- 42 H. Fu, H. Gao, G. Wu, Y. Wang, Y. Fan and J. Ma, *Soft Matter*, 2011, **7**, 3546–3552.
- 43 X. Jiang, J. Li, M. Ding, H. Tan, Q. Ling, Y. Zhong and Q. Fu, *Eur. Polym. J.*, 2007, **43**, 1838–1846.
- 44 O. Belaidi, T. Bouchaour and U. Maschke, *Org. Chem. Int.*, 2013, 2013, 348379–348392.
- 45 F. Tamimi, J. Torres, R. Bettini, F. Ruggera, C. Rueda, M. L. Ponce and E. L. Cabarcos, *J. Biomed. Mater. Res. A.*, 2008, **85**, 707–714.
- 46 P. Mastorakos, E. Song, C. Zhang, S. Berry, H. W. Park, Y. E. Kim, J. S. Park, S. Lee, J. S. Suk and J. Hanes, *Small*, 2016, **12**, 678–685.
- 47 J. Ko, K. Park, Y. S. Kim, M. S. Kim, J. K. Han, K. Kim, R. W. Park, I. S. Kim, H. K. Song, D. S. Lee and I. C. Kwon, *J. Control. Release*, 2007, **123**, 109–115.
- 48 D. M. Brey, J. L. Ifkovits, R. I. Mozia, J. S. Katz and J. A. Burdick, *Acta Biomater.*, 2008, **4**, 207–217.
- 49 S. Farris, L. Introzzi, P. Biagioni, T. Holz, A. Schiraldi and L. Piergiovanni, *Langmuir*, 2011, **27**, 7563–7574.
- 50 D. L. Safranski, J. C. Crabtree, Y. R. Huq and K. Gall, *Polymer*, 2011, **52**, 4920–4927.
- 51 H. Fu, H. Gao, G. Wu, Y. Wang, Y. Fan and J. Ma, *Soft Matter*, 2011, **7**, 3546–3552.
- 52 B. Amsden, *Soft Matter*, 2007, **3**, 1335–1348.
- 53 X. Z. Zhang, D. Q. Wu and C. C. Chu, *J. Polym. Sci. Polym. Phys.*, 2003, **41**, 582–593.
- 54 B. Tasdelen, N. K. Apohan, O. Guven and B. M. Baysal, *J. Appl. Polym. Sci.*, 2004, **91**, 911–915.
- 55 Y. G. Lee, H. S. Kang, M. S. Kim and T. Son, *J. Appl. Polym. Sci.*, 2008, **109**, 3768–3775.
- 56 R. S. Wong, M. Ashton and K. Dodou, *Pharmaceutics*, 2015, **7**, 305–319.
- 57 T. Etrych, V. Subr, R. Laga, B. R. Ihova and K. Ulbrich, *Eur. J. Pharm. Sci.*, 2014, **58**, 1–12.
- 58 S. L. Elliott, J. D. Fromstein, J. P. Santerre and K. A. Woodhouse, *J. Biomater. Sci. Polym. Ed.*, 2002, **13**, 691–711.
- 59 A. J. Domb, J. Kost and D. Wiseman, *Handbook of Biodegradable Polymers*, CRC Press, Amsterdam, 1998.
- 60 E. Pamuła, M. Błażewicz, C. Paluszkiwicz and P. Dobrzyński, *J. Mol. Struct.*, 2001, 596, 69–75.
- 61 J. B. Wolinsky, Y. L. Colson and M. W. Grinstaff, *J. Control. Release*, 2012, **159**, 14–26.
- 62 R. S. Labow, E. Meek, L. A. Matheson and J. P. Santerre, *Biomaterials*, 2002, **23**, 3969–3975.
- 63 W. Song, Z. Tang, M. Li, S. Lv, H. Yu, L. Ma, X. Zhuang, Y. Huang and X. Chen, *Macromol. Biosci.*, 2012, **12**, 1375–1383.
- 64 C. Yanga, Z. Xuea, Y. Liua, J. Xiaoa, J. Chena, L. Zhangb, J. Guoa and W. Lina, *Mater. Sci. Eng. C*, 2018, **84**, 254–262.
- 65 J. Wang, B. M. Wang, and S. P. Schwendeman, *J. Control. Release*, 2002, **82**, 289–307.
- 66 J. E. Bryant, M. P. Brown, R. R. Gronwall and K. A. Merritt, *Equine Vet. J.*, 2000, **32**, 233–238.
- 67 M. Donbrow and Y. Samuelov, *J. Pharm. Pharmacol.*, 1980, **32**, 463–470.
- 68 M. Gibaldi and S. Feldman, *J. Pharm. Sci.*, 1967, **56**, 1238–1242.
- 69 N. A. Peppas, *Pharm. Acta Helv.*, 1985, **60**, 110–111.
- 70 P. L. Ritger and N. A. Peppas, *J. Control. Release*, 1987, **5**, 23–36.
- 71 R. Das and S. Pal, *Colloids Surf. B.*, 2013, **110**, 236–241.
- 72 R. W. Korsemeyer, R. Gurny, E. Doelker, P. Buri, and N. A. Peppas, *Int. J. Pharm.* 1983, **15**, 25–35.
- 73 M. Kopcha, N. G. Lordi and K. J. Toja, *J. Pharm. Pharmacol.*, 1991, **43**, 382–387.
- 74 T. Higuchi, *J. Pharm. Sci.* 1961, **50**, 874–875.
- 75 A. W. Hixson and J. H. Crowell, *Ind. Eng. Chem.*, 1931, **23**, 923–931.
- 76 A. Thakur, S. Monga, and R. K. Wanchoo, *Chem. Biochem. Eng. Q.*, 2014, **28**, 105–115.
- 77 B. Tasdelen, N. K. Apohan, O. Guven and B. M. Baysal, *J. Appl. Polym. Sci.*, 2004, **91**, 911–915.